

# Insights from the great 2011 Japan earthquake

Thorne Lay and Hiroo Kanamori

The diverse set of waves generated in Earth's interior, oceans, and atmosphere during the devastating Tohoku-oki earthquake reveal some extraordinary geophysics.

On 11 March 2011, the nation of Japan and geophysicists around the world received a terrible surprise: A huge earthquake, significantly stronger than people had anticipated or prepared for in the region, struck off the northeastern shore of Honshu. Shear sliding on the fault where the Pacific Plate thrusts below Japan lasted for 150 anxiety-filled seconds, shifted the coast of Japan up to 5 m eastward, and lifted the sea floor by as much as 5 m over 15 000 km<sup>2</sup>, an area comparable to the state of Connecticut.<sup>1,2</sup> Displacements as large as 60 to 80 m—the largest ever measured for an earthquake—occurred near the subduction trench, and a total strain energy equivalent to a 100-megaton explosion was released during the sliding. This was the great 2011 Tohoku-oki earthquake, so-named for the region it struck, shown in figure 1.

The sudden sea-floor displacement generated a massive tsunami that swept onto hundreds of kilometers of coastline along the islands of Honshu and Hokkaidō. Tsunami waves 3–15 m high overtopped harbor-protecting tsunami walls and coastal margins and penetrated as far as 10 km inland along the coastal plain.<sup>3</sup> The flood destroyed many small towns and villages, killed some 20 000 people, and initially displaced nearly half a million; six months later, tens of thousands were still living in high school gymnasiums and other temporary quarters (see PHYSICS TODAY, November 2011, page 20). The high waves also disrupted the power supply needed to maintain water circulation for cooling the reactors at the Fukushima nuclear power plant, which precipitated a catastrophic release of radiation that continues to plague central Japan.

Located along the Pacific Ring of Fire, Japan has experienced a long history of earthquakes, but the Tohoku-oki quake was a rare giant with no instrumentally recorded precedent. Researchers estimate its moment magnitude  $M_w$  at 9.0. (To appreciate that

measure of radiated seismic energy, see box 1.) The huge event abruptly released elastic strain energy that had accumulated in the rocks on either side of the shallow-dipping plate boundary—the megathrust fault—for more than a millennium since the last great earthquake in the central part of the megathrust, which occurred in 869 with  $M_w \geq 8.3$ . (Another large earthquake occurred in 1611 near the northern part of the 2011 rupture zone, but its details are murky and still debated.)

The strain release generated seismic, tsunami, and atmospheric waves that spread through Earth. Those wave phenomena were captured by thousands of geophysical facilities worldwide, including dense Japanese networks of seismic and GPS stations deployed after the devastating 1995 Kobe earthquake, and by the large numbers of tsunami gauges and deepwater pressure sensors deployed near Japan and across the Pacific Ocean following the Sumatra–Andaman earthquake and tsunami in December 2004 (see PHYSICS TODAY, June 2005, page 19). Combined with extensive recordings from global seismic networks, the data from those stations, gauges, and sensors make the 2011 Tohoku-oki event the best-recorded earthquake and tsunami in history.<sup>1,4</sup>

## Plate-boundary physics

Great earthquakes are those whose moment magnitudes are 8.0 or higher. Their activity varies significantly between different subduction zones. Some subduction zones—for example, ones in southern Chile, Sumatra, and southwestern Japan—produce repeated, great-earthquake ruptures every century or two, while others—in the Mariana Islands and Tonga, say—produce them rarely, if ever.

**Thorne Lay** and **Hiroo Kanamori** are seismologists at the University of California, Santa Cruz, and the California Institute of Technology in Pasadena, respectively.

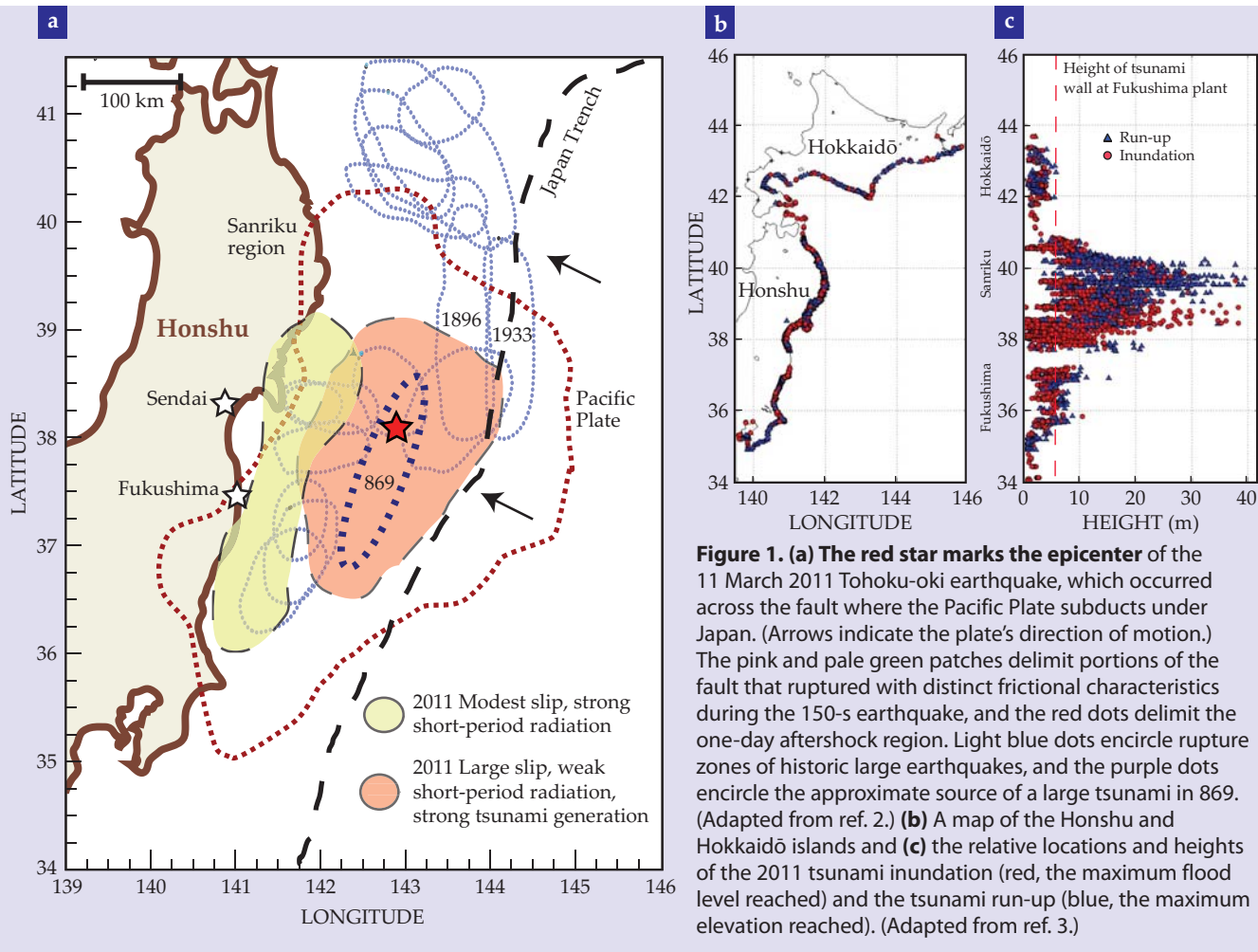


**Figure 1.** (a) The red star marks the epicenter of the 11 March 2011 Tohoku-oki earthquake, which occurred across the fault where the Pacific Plate subducts under Japan. (Arrows indicate the plate's direction of motion.) The pink and pale green patches delimit portions of the fault that ruptured with distinct frictional characteristics during the 150-s earthquake, and the red dots delimit the one-day aftershock region. Light blue dots encircle rupture zones of historic large earthquakes, and the purple dots encircle the approximate source of a large tsunami in 869. (Adapted from ref. 2.) (b) A map of the Honshu and Hokkaido islands and (c) the relative locations and heights of the 2011 tsunami inundation (red, the maximum flood level reached) and the tsunami run-up (blue, the maximum elevation reached). (Adapted from ref. 3.)

That variability is attributable to differences in plate-boundary frictional characteristics, illustrated in figure 2. Dark patches represent seismic portions of the fault surface where the slip generates earthquakes, and white patches represent areas where the slip is primarily aseismic—slowly sliding without earthquakes. At shallow depths, the seismic patches can rupture as tsunami earthquakes—a name reserved for large, tsunami-generating events that, because of unusually low rupture-expansion rates, occur without generating strong, short-period seismic waves. Conditionally stable regions normally slip continuously but can also slip seismically when loaded abruptly during the failure of neighboring seismic patches.

The ratio of the area of seismic patches to the total area of the fault is large for subduction zones with frequent great earthquakes and small for zones with infrequent great earthquakes. Depending on how regions of the megathrust with different rupture characteristics fail, though, diverse earthquake sequences are possible. A failure of one seismic patch may produce a single, large earthquake. But when two or more patches fail in a cascade that also prompts conditionally stable regions between them to slip seismically, the result is a much larger earthquake than one would otherwise expect from just

the seismic patches alone. An example of such behavior has been observed for a great earthquake that occurred along the Ecuador–Colombia coast in 1906.

The Tohoku-oki subduction zone is thought to comprise a mixture of such seismic and aseismic patches and a concomitant mix of frictional characteristics that can lead to an unusual diversity of rupture patterns. Subregions slide aseismically around localized patches that fail repeatedly in a number of ways—as frequent small earthquakes; as moderate-sized earthquakes accompanied by large amounts of slow, postseismic slip of a few centimeters per day instead of the typical kilometers-per-second rate of an earthquake rupture; or as shallow tsunami earthquakes.<sup>1,5</sup>

The shallow portion of the megathrust just north of the 2011 earthquake zone and illustrated in figures 1a and 2b ruptured during the great 1896 ( $M_w$  about 8.2) tsunami earthquake. The Pacific Plate in that region also experienced an internal rupture in 1933 from extension near the Japan trench. Similarly large megathrust earthquakes within the 2011 rupture zone during the past century all occurred near the coast, but the region farther offshore where large slip occurred in the 2011 event was known to have previously ruptured only in the 869

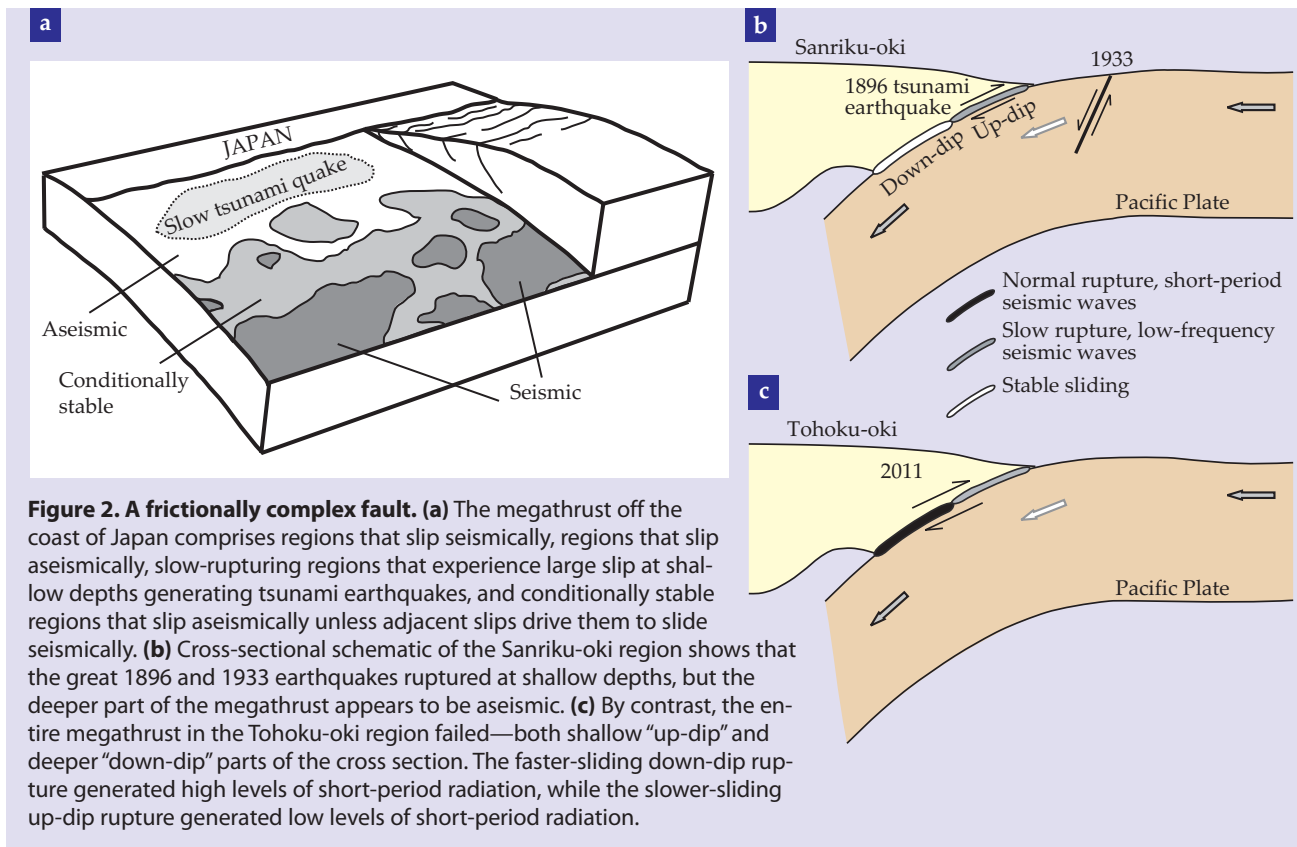


**Figure 2. A frictionally complex fault.** (a) The megathrust off the coast of Japan comprises regions that slip seismically, regions that slip aseismically, slow-rupturing regions that experience large slip at shallow depths generating tsunami earthquakes, and conditionally stable regions that slip aseismically unless adjacent slips drive them to slide seismically. (b) Cross-sectional schematic of the Sanriku-oki region shows that the great 1896 and 1933 earthquakes ruptured at shallow depths, but the deeper part of the megathrust appears to be aseismic. (c) By contrast, the entire megathrust in the Tohoku-oki region failed—both shallow “up-dip” and deeper “down-dip” parts of the cross section. The faster-sliding down-dip rupture generated high levels of short-period radiation, while the slower-sliding up-dip rupture generated low levels of short-period radiation.

earthquake, which produced a large tsunami inundation along the coast near Sendai. Even given Japan’s exceptionally long historical record of earthquakes, researchers’ evaluations of the region’s earthquake potential are complicated by the range of sliding behavior along the megathrust and the wide spans of time—from a few years to many centuries—for distinct parts of it to repeatedly slip. The rupture of the 2011 earthquake involved many of those parts failing in a cascade that had not been anticipated in any of the seismic hazard models for the region.

Over the 15 years prior to 2011, a network of GPS stations (now numbering more than 1200) across Japan detected a gradient of westward displacements decreasing from east to west across the island of Honshu. Several groups had modeled that compressional crustal strain by assuming that the offshore plate-boundary fault was locked, unable to slip to varying degrees as the plates converged, as suggested in figure 3. Although the offshore region to the north experienced little of that locking, the deeper portion of the megathrust where the 2011 event subsequently occurred was found to be not slipping at all. Even so, most studies assumed that the “up-dip” part of the fault—that is, the shallow part of it—was not accumulating strain.<sup>6</sup>

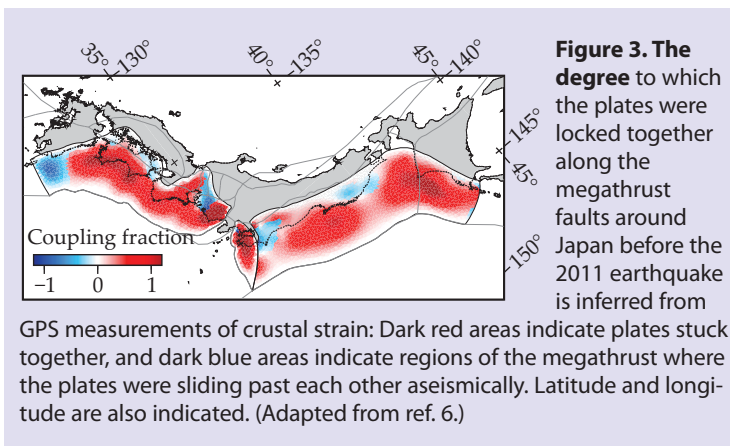
In recent years new technologies have emerged for tracking ground positions offshore using ocean-bottom GPS sensors, and data were beginning to demonstrate that the up-dip part of the megathrust was accumulating strain. Indeed, that surprisingly strong part of the fault, which had loaded up strain

for more than a millennium without rupturing, suddenly overcame frictional resistance on 11 March 2011. Given a few more years of offshore strain measurements before the earthquake struck, it is likely that the potential for so great an event would have been clearer.

### Making waves

Abrupt sliding of the strongly locked region of the megathrust released elastic strain energy from the rock, which drove the rupture, heated the fault, and generated both seismic waves and permanent deformation in the rock around the fault. As the fault slipped, elastic compressional and transverse seismic waves—known as *P* and *S* waves, respectively—spread outward in all directions. Rebound of the elastic deformation of the rock, in turn, shifted the Japan mainland eastward and uplifted the ocean floor. The many gigatons of displaced ocean water generated tsunami waves, and the seismic and tsunami-wave energy coupled to the atmosphere to produce yet more waves, all spreading from the source with different velocities. The entire Earth system was perturbed by the energy release, and the total mass redistribution reduced the length of an Earth day by about 1.8 microseconds. (For a primer on the physics behind the processes, see the essay by David Stevenson in *PHYSICS TODAY*, June 2005, page 10.)

Seismic waves shook the ground in Japan with a high frequency of about 10 Hz, ground accelerations as large as 2.7 *g*, and peak ground velocities of 80 cm/s across Honshu. At the Fukushima nuclear



power station, the shaking rose 20% higher than the 0.45-g level the station was designed to tolerate, but because of the subsequent explosions at the facility it is unclear how much damage was inflicted from the shaking. Despite the strong shaking along the coast, many structures had only moderate or light damage, a testament to Japan's effective building codes and construction standards.

Several thousand seismometers in Japan's networks of short-period and broadband seismic stations recorded the ground vibrations, and continuously recording GPS stations made 1200 additional measurements of the transient and static ground motions.<sup>17</sup> The seismic waves propagated through Earth and were captured by some 1300 broadband global seismometers, many of which transmitted the data in near-real time to collection centers; the immediate availability of data facilitated rapid analysis of the signals by seismologists around the world.<sup>1,5,8</sup>

The local recordings in Japan formed the basis for the Japan Meteorological Agency's tsunami

### Box 1. Moment magnitude

There are many measures of earthquake size, but overall faulting significance is best captured by seismic moment,  $M_0 = \mu AD$ , where  $\mu$  is the shear rigidity of rock around the fault,  $A$  is the total rupture area that slides, and  $D$  is average slip—that is, the displacement of one side of the fault relative to the other. Expressed in Newton meters, the seismic moment directly determines the strength of low-frequency seismic waves generated by an earthquake. The moment magnitude,  $M_w = (\log M_0 - 9.1)/1.5$ , is now a widely used magnitude measure based on the seismic moment, which is accurately measured by modeling low-frequency seismic recordings during an event. The seismic moment increases by a factor of about 31.6 for each unit increase in  $M_w$ . The largest recorded earthquake in history was the 1960 Chile earthquake with  $M_w = 9.5$ . The 2011 Tohoku-oki earthquake was found to have a seismic moment of  $2.9 \times 10^{22}$  Nm, which gives  $M_w = 9.0$ , somewhat lower than the 1964 Alaska ( $M_w$  9.2) and 2004 Sumatra–Andaman ( $M_w$  9.2) earthquakes, ranking it the fourth largest event since the era of seismological recordings began in the early 1900s.

warning within three minutes from the start of the rupture (see box 2). Numerous gauges and tide meters measured the tsunami as it approached and rushed over the coast. And though some sensors were driven off-scale, several complete recordings document the wave, exemplified in figure 4a.

A narrow pulse-like waveform is apparent in the wave recorded off the coast of Iwate Prefecture (Sanriku), where run-up was greatest. That peak arrived about 20 minutes after the faulting began, consistent with the sea-floor uplift in a narrow zone near the Japan trench. Tsunamis travel slowly in shallow coastal water, and many people were able to reach high ground in time to escape the flooding.

The tsunami spread seaward as well.<sup>9</sup> As waves spread through the northern Pacific, their 20-minute period and meter-high amplitudes were recorded by numerous Deep-Ocean Assessment and Reporting of Tsunamis buoys operated by the US National Oceanic and Atmospheric Administration. NOAA analyzed those signals quickly enough to accurately predict the waves' arrival times and amplitudes at Pacific island coastlines. Greatly expanded since 2004, the buoy system worked superbly, and the deepwater signals have been incorporated into studies of the rupture process.<sup>1,3</sup>

The tsunami struck Hawaii about 7 hours after the earthquake—and the coast of California 3 hours later still—with enough force to damage harbors, marinas, and coastal resorts. The Philippines, Indonesia, and New Guinea suffered significantly. And minor damage occurred in Peru and Chile when the wave struck their coastlines 20 to 22 hours after the event.

The combined motions in the rocks and ocean produced atmospheric waves, which extended the reach of the great earthquake to a planetary scale. Those waves became amplified with altitude as atmospheric density decreased and created large perturbations in the ionosphere. The coupling of Earth's solid, liquid, and gaseous layers is generally well understood, and the atmospheric waves were widely recorded by barometric pressure sensors at the surface. GPS stations around Japan sensed the ionospheric perturbations due to their effects on the transmission of satellite radio signals.<sup>10</sup> The ionospheric disturbance involved fluctuating electron density up to altitudes of 350 km caused by atmospheric waves expanding from the source at 720–800 km/hr.

The main shock of the Tohoku-oki earthquake produced extensive aftershock activity in both the upper and lower plates and in regions of the megathrust laterally adjacent to the main rupture zone. Within 24 hours hundreds of aftershocks had occurred over an area 500 km long and 300 km wide. Many resulted from extensional faulting in the upper plate, indicative of the large strain relaxation that occurred when the fault slipped.

Many minor faults within Japan's crust were activated by the change in stress from the main event.<sup>11</sup> Extensive regions of the upper 100 m of Japan's crust experienced ephemeral reductions in seismic shear velocity, likely as a result of shaking-induced cracking and the movement of ground-

water.<sup>12</sup> Ongoing research is quantifying the broad reach of the stress perturbations from the great event.

## Rupture physics

Armed with extensive geophysical recordings of ground, ocean, and atmosphere before, during, and after the 2011 earthquake, researchers can study its rupture physics closely. Although reports of possible precursory phenomena exist—for instance, IR heating of the atmosphere above the source region several days before the event and anomalous total-electron readings of the ionosphere preceding the earthquake—no clear deformational precursor has emerged from analyses of the geodetic and seismic data sets.

There were earthquakes, now identified as foreshocks, for several days before the main shock; the largest was an  $M_w$  7.5 on 9 March 2011. Their importance as harbingers is again unclear, but they were clustered near the point of initiation of the main shock and plausibly represent accelerating deformation in that region. The weak initial onset of the rupture raises many questions about how it grew so huge.

According to analyses of the data, the main rupture spread on the fault with relatively low expansion velocity of about 1 km/s, initially expanding for about 50 s “down-dip”—that is, deep within the fault—toward the coast near Sendai, where numerous large earthquakes have occurred this past century and earlier, as outlined in light blue in figure 1a. The rupture then expanded into shallower depths for the next 40 s, with the largest slip along the fault occurring more than 150 km offshore, close to the trench. That part of the rupture, in turn, was followed by additional sliding down-dip that migrated southward along the coastline at about 2.5 km/s.

The slip near the trench was enormous; it averaged about 40 m over the upper 100 km of the megathrust and peaked at 60–80 m close to the trench.<sup>1,5,13</sup> Those are the largest fault displacements documented for any earthquake in history. Using elastic dislocation theory to predict the sea-floor uplift, one can accurately account for the size of the tsunami from geophysical fault models. But ongoing research is evaluating whether any nonelastic deformations, such as submarine landslides, were also involved.

Researchers estimate a stress drop of 15–30 MPa in that large-slip region, significantly greater than the few-MPa stress drops typically found for large interplate ruptures. Seismic imaging of rock around the shallow fault zone reveals relatively high  $P$ -wave velocities and some seaward arching of the upper plate toward the trench. Those data suggest the presence of hard, strong, and brittle rock around the fault, at odds with conventional belief that the shallowest regions of subduction zones are weak and deform mainly anelastically.<sup>14</sup>

The dense seismic observations of the Earth-Scope Transportable Array in North America reveal that strong coherent bursts of short-period radiation, which likely produced the violent shaking in

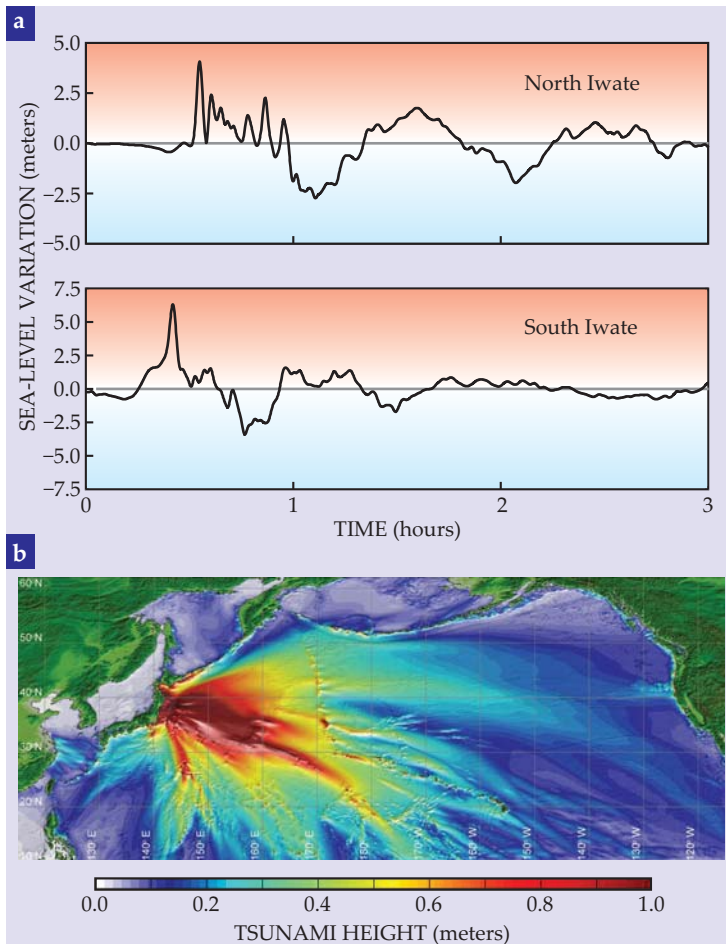


**Figure 4.** Several tsunami gauges just off Japan’s Pacific coastline record sea-level variations. **(a)** Measurements from GPS gauges offshore north and south Iwate in the Sanriku region show the waveform as the tsunami reached each station 20–30 minutes after the earthquake struck. The narrow, large-amplitude peak at each station originated near the Japan trench and produced up to 40-m run-up heights along the coastline. **(b)** The tsunami also spread out to sea, its peak amplitude gradually diminishing across the deep Pacific Ocean, as calculated for a faulting model derived from seismic waves. (This issue’s cover shows similar calculated tsunami amplitudes from modeling buoy data.) The tsunami reached California about 10 hours after the earthquake. (Adapted from ref. 9.)

Honshu, preferentially emanated from the deeper half of the megathrust, where total slip was much smaller than in the upper part of it.<sup>15</sup> In that respect, the shallow rupture in the 2011 earthquake behaved much like the shallow tsunami earthquake of 1896. But the huge shallow slip, 50–90 s after the earthquake began, appears to have driven the central, deep portion of the fault to rerupture and slip along adjacent regions of conditional stability, which accentuated the total size and energy.

Thus the 2011 earthquake was essentially a composite event, as discussed earlier, with attributes of a tsunami earthquake for the shallow portion of the rupture and attributes of a typical megathrust earthquake in the deeper portion of it. The great

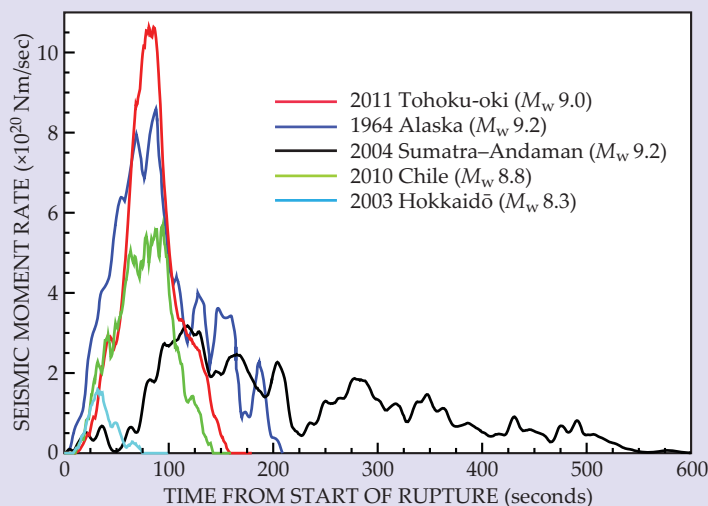


**Figure 5. Seismic moment rate functions (MRFs),** plotted for several great earthquakes. MRF measures the time rate of change in seismic moment—the product of the surrounding rock’s rigidity, the fault area, and the slip—and is roughly proportional to the rate of energy radiation. The large, smooth, and narrow MRF for the Tohoku-oki earthquake reflects the unusually large slip that occurred over a small localized region. The Sumatra–Andaman earthquake, by contrast, occurred for a much longer duration, and its extended MRF reflects the spatially separated slip patches along the Sumatra, Nicobar, and Andaman islands. The MRF of the Alaska earthquake has a character between those extremes. The Chile earthquake lasted nearly as long as the Tohoku-oki event, but with much smaller peak MRF and possibly shorter-period fluctuations, which suggest different frictional characteristics between the regions’ faults. Finally, the far smaller MRF of the Hokkaidō earthquake illustrates the vast differences in radiated energy and tsunami hazard that distinguish  $M_w$  8 and 9 earthquakes.

2004 Sumatra rupture was similarly enhanced by extending over multiple subregions. The behavior points to a weakness of the “characteristic earthquake” model often used for probabilistic seismic hazard assessment.

The seismic moment estimated for the main shock is  $M_0 = 2.9 \times 10^{22}$  Nm, and the total radiated energy release is  $4.2 \times 10^{17}$  J. But the most robust aspect of the earthquake determined from seismology is the moment rate function, which characterizes the source strength for seismic wave motions generated during the faulting. The comparison in figure 5 of the moment rate function from Tohoku-oki with that of other 20th-century great earthquakes reveals the 2011 event’s distinctly high peak and short duration. Indeed, by that measure, Tohoku-oki re-

leased a larger peak energy per unit time than any earthquake ever recorded.

### Lessons learned

Earth has experienced a high rate of great earthquakes during the past decade—about 2.5 times the average rate for the past century.<sup>15</sup> Fortunately, the expansion and improvement of geophysical recordings enable geoscientists to learn from each one. The 11 March 2011 Tohoku-oki earthquake demonstrated that shallow portions of megathrust faults can support higher stresses and accumulate larger strains than conventional wisdom had suggested. Thus tsunami earthquakes, or composite events like the recent one in Japan, may occur more broadly than researchers had thought.

## Box 2. Tsunami and earthquake warning

In recent years the Japan Meteorological Agency (JMA) has made significant improvements to its tsunami warning system. On the basis of its preliminary seismic magnitude estimate, 7.9, JMA issued a warning just 2 minutes and 40 seconds after the Tohoku-oki earthquake began. The agency warned that 6-m, 3-m, and 3-m tsunamis could be expected along the coast of Miyagi, Iwate, and Fukushima prefectures, respectively. Undoubtedly, that saved thousands of lives because the largest tsunami did not reach the coast until about 20 minutes after the earthquake began.

However, some reports indicate that many people did not take immediate action out of a belief that the extensive network of tsunami walls would protect them. Given a more accurate early estimate of the true enormity of the event,  $M_w = 9$ , the JMA would have been able to issue a warning that might have prompted more extensive evacuations. Methods have been developed to correctly assess an earthquake’s magnitude and

faulting geometry within minutes of its occurrence; unfortunately, those methods had not yet been implemented in Japan’s operational system.

The JMA also operates an earthquake early warning system. Earthquake warning is more challenging than tsunami warning as it relies on the initial seismic vibrations to gauge the likely level of ensuing shaking. But the initial 5–10 seconds of shaking produced by the Tohoku-oki earthquake was weak, comparable to a magnitude 4.9 event, and the JMA’s earthquake early warning system underestimated the expected overall intensity. Nevertheless, the information was useful for some. It wasn’t the only early warning system available. The Japanese bullet train network, for instance, had its own warning system. More than 20 bullet trains were running at high speed in the Tohoku district when the earthquake struck. But within a few seconds of detecting the primary seismic wave, the warning system shut down the power and stopped all the trains without incident.

Moreover, the accumulating examples of tsunami events—documented in the Aleutian Islands, Peru, Sumatra, Java, the Kuril Islands, and now Japan—are persuasive evidence that even relatively long seismological records are too limited to adequately assess the hazard from infrequent but devastating events. Fortunately, the great progress in geodesy to map out regions of strain accumulation near subduction zones makes it a major new tool for evaluating seismic potential. But clearly, more off-shore geodetic measurements will be particularly valuable. In any case, the continued investigation of many regions is perhaps the best strategy for coping with a limited historical record.

The complex variations of slip behavior on the Japan megathrust highlight our ignorance of what controls fault behavior. How pressure, temperature, fluids, rock composition, and other factors influence the variations in slip rates and seismic radiation over a fault remains to be quantified. Progress requires dense onshore and offshore data collection and concerted investigation of regions of concern such as along the Cascadia margin off the coast of Oregon and Washington where a major research effort is under way.

The Tohoku-oki event confirmed the value of applying modern technologies to earthquake and tsunami mitigation efforts. Strain-accumulation measurements, offshore fault-zone observations, and early earthquake and tsunami warning systems all played a role in saving lives, as terrible as the event was. Extreme events can and do happen, and resources may be too limited to fully protect ourselves. Our best prospect for coping with those events' effects, however, is to draw on our technologies, preparations, and ability to respond when Earth delivers the unexpected, as it did on 11 March 2011.

*We thank many colleagues who have shared information about the great Tohoku-oki earthquake summarized here and thank NSF for supporting research on this event with grant EAR0635570.*

## References

1. H. Kanamori, K. Yomogida, eds., Special issue: "First Results of the 2011 Off the Pacific Coast of Tohoku Earthquake," *Earth Planets Space* **63**, 511 (2011).
2. K. D. Koper et al., *Earth Planets Space* **63**, 599 (2011).
3. Japan Society of Civil Engineers Tohoku Earthquake Tsunami Information, <http://www.coastal.jp/tsunami2011/index.php>.
4. M. Sato et al., *Science* **332**, 1395 (2011).
5. M. Simons et al., *Science* **332**, 1421 (2011).
6. J. P. Loveless, B. J. Meade, *J. Geophys. Res.* **115**, B02410 (2010).
7. S. Ozawa et al., *Nature* **475**, 373 (2011).
8. S. Ide, A. Baltay, G. C. Beroza, *Science* **332**, 1426 (2011).
9. Y. Yamazaki et al., *Proceedings of Oceans '11 MTS/IEEE Kona*, IEEE, Piscataway, NJ (in press).
10. A. Saito et al., *Earth Planets Space* **63**, 863 (2011).
11. S. Toda, R. S. Stein, J. Lin, *Geophys. Res. Lett.* **38**, L00G03 (2011).
12. N. Nakata, R. Snieder, *Geophys. Res. Lett.* **38**, L17302 (2011).
13. H. Yue, T. Lay, *Geophys. Res. Lett.* **38**, L00G09 (2011).
14. D. Zhao et al., *Geophys. Res. Lett.* **38**, L17308 (2011).
15. C. J. Ammon, T. Lay, D. W. Simpson, *Seismol. Res. Lett.* **81** (1), 965 (2010). ■



**search  
SMARTER**

Find the supplies and services you need using a network that physicists trust — without the unrelated clutter of the large search engines.

Start your search today at:  
**[physicstodaybuyersguide.com](http://physicstodaybuyersguide.com)**

**physics  
today**